ELSEVIER

Solid State Ionics 131 (2000) 13–22

SOLID STATE IONICS

www.elsevier.com/locate/ssi

Point-defect thermodynamics and size effects

Joachim Maier*

Max-Planck-Institut für Festkörperforschung, Heisenbergstraße 1, 70569 Stuttgart, Germany

Received 30 June 1998; received in revised form 15 July 1998; accepted 15 July 1998

Abstract

The introductory part reviews some basic aspects of bulk point-defect thermodynamics. It makes use of the fact that for the purposes under consideration, the real structure can be decomposed in a perfect ground structure and a superimposed defect structure. Then modifications of the point-defect concentration and distribution are considered occurring if interfaces are approached. A simple treatment is possible for the abrupt core-space charge situation in which the standard chemical potentials are assumed to change in a step-like way. Evidence is given that in very many cases this is a reasonable model. There, the adjustment at interfaces occurs solely via space charge regions. 'Trivial' size effects are brought about by the changed surface (i.e. core plus space charge layer) to volume ratio. A mesoscale size effect is expected if the width of the space charge layers is no longer small compared with the distance of neighbouring interfaces (Debye-length λ as scaling parameter). In some situations, e.g. if extremely small clusters are treated, distinct deviations in the ground structure also occur, affecting energetic and entropic standard terms. Since such modifications usually decay steeply with increasing interfacial distance (L), another scaling parameter (ℓ) defines a further mesoscopic regime. As examples, micro- and nano-sized particles, films, polycrystals and composites are discussed.

Keywords: Point defects; Thermodynamics; Size effects; Interfaces; Space charges; Nanocrystallinity

1. Introduction

Point defects in solids are, on the one hand, analogous to the H_3O^+ and OH^- ions which play a central role in aqueous electrochemistry, and to excess electrons and electron holes, the decisive carriers in semiconductor physics, on the other. In both fields it is a matter of fact that boundary effects have a significant influence on the charge carrier concentrations and distributions.

In both fields, the importance of the nanoscale is also evident as exemplified by colloid chemistry, bio-electrochemistry [1–3] or by the emerging field of nano-electronics [4]. Beyond that, the nanoscale is the scale on which macroscopic and microscopic concepts meet, e.g. the transition between cluster chemistry and physics [5–7], and solid state science.

In this contribution, static interfacial effects are discussed for the field of Solid State Ionics in particular with respect to expected and observed nanosize phenomena (cf. also Refs. [8–10]).

The structure of the paper is as follows: After a brief overview on bulk defect thermodynamics (Section 2), the defect chemistry at interfaces embedded

*Tel.: +49-711-689-1720; fax: +49-711-689-1722.

E-mail address: weiglein@chemix.mpi-stuttgart.mpg.de (J. Maier)

0167-2738/00/$ – see front matter
PII: S0167-2738(00)00618-4

in the infinite bulk is considered (Section 3). In Section 4 interfaces are successively brought closer to each other and the resulting size effects are studied.

2. Point-defect thermodynamics in the infinite bulk

In the classical treatment of defective materials, the real structure is decomposed into a perfect (ground) structure and a (chemically excited) defect structure:

Real structure = perfect structure + defect structure (1)

the first one being invariant while the latter responds to changes in the state and control parameters, in particular temperature (T), doping content (C) and component potential (e.g. expressed by the oxygen partial pressure P in a binary oxide). In the infinite bulk, electroneutrality is usually an excellent assumption [11–13]. Global and local equilibrium at constant T and total pressure demands the minimisation of the Gibbs energy in terms of the particle numbers. If the defects are dilute, Boltzmann statistics can be applied and ideal mass action laws follow. If the electroneutrality condition can be condensed to a proportionality of two majority carrier concentrations, the power law form [14–16]

$$c_j = \alpha_j P^{N_j} C^{M_j} \Pi_T K_r^{\gamma_{rj}}(T) \quad (2)$$

results, with the characteristic exponents N_j, M_j, γ_{rj} (simple rational numbers). The K_rs are the mass action constants of the defect reactions under regard. Representations of $\log c_j$ *vs.* $\log P$ (Kröger–Vink plots), $\log c_j$ vs. $\log C$ as well as $\log c$ vs. $1/T$ (Arrhenius or better van't Hoff plots) yield straight lines with N_j, M_j and $\Sigma_r \gamma_{rj}\Delta_r H^\circ$ ($\Delta_r H^\circ$: standard enthalpy of reaction r) as slopes. A sensitive measure for c_j is the conductivity σ_j which also involves the T-dependent mobility.

Fig. 1 shows the defect chemistry of the Frenkel disordered material AgCl. Since ionic carriers are in majority, the electroneutrality equation is $[Ag_i^\cdot] \simeq [V'_{Ag}]$. The important disorder reactions are the Frenkel reaction (r=F)

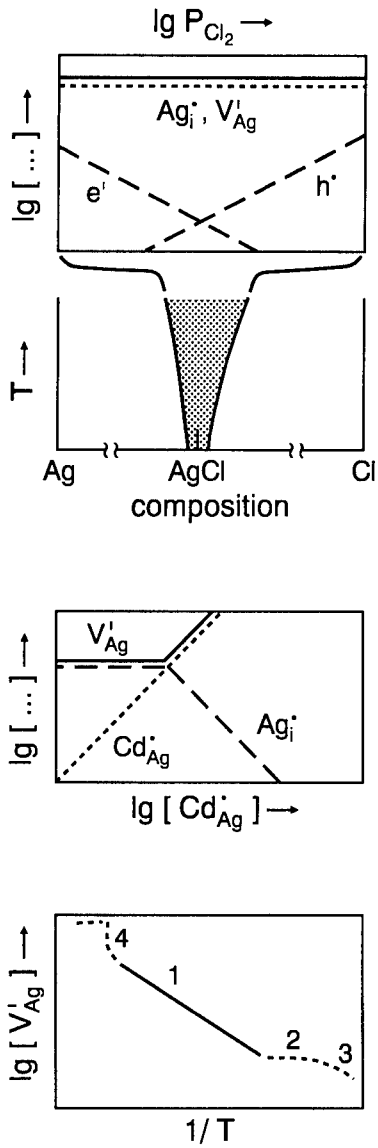

Fig. 1. Defect chemistry in the bulk of AgCl.

$$Ag_{Ag} + V_i \rightleftharpoons Ag_i^\cdot + V'_{Ag} \quad (3)$$

as well as the interaction with the component potential according to (r=Cl)

$$\frac{1}{2}Cl_2(g) + Ag_i^\cdot \rightleftharpoons AgCl + V_i + h^\cdot \quad (4)$$

or in terms of Ag (g) (r=Ag)

$$Ag(g) + h^\cdot + V_i \rightleftharpoons Ag_i^\cdot. \quad (5)$$

Note that silver and Cl_2-partial pressures are related to the formation enthalpy according to

$$P_{Ag} \cdot P_{Cl_2}^{1/2} \simeq \text{const.} \exp - \Delta_f G_{AgCl}^{\circ}. \quad (6)$$

The inter-correlation of $[h^{\cdot}]$ with $[e']$ is provided by the band gap transfer (r=B)

$$\text{Nil} \rightleftharpoons e' + h^{\cdot}. \quad (7)$$

The interaction with the component potential is only relevant on the level of the electrons as minority carriers, while the majority carrier concentrations (ions) are approximately independent of P_{Cl_2} and P_{Ag}. Hence, $[Ag_i^{\cdot}] = [V'_{Ag}] = K_F^{1/2}$ as shown at the top of Fig. 1, while $[e'](\propto P_{Cl_2}^{-1/2})$ and $[h^{\cdot}](\propto P_{Cl_2}^{1/2})$ sensitively depend on the position in the phase diagram. In the van't Hoff diagram (bottom of Fig. 1), a straight line (1) results with the slope of $\Delta_F H^{\circ}/2$.

Irreversibly introduced aliovalent impurity traces (e.g. Cd^{2+} on Ag^+-site, i.e. $Cd_{Ag}^{\cdot}$) appear in the electroneutrality equation only. If $[Cd_{Ag}^{\cdot}]$ has been increased to values in the order of or greater than $K_F^{1/2}$ (see centre Fig. 1), $[V'_{Ag}]$ increases $(\rightarrow [Cd_{Ag}^{\cdot}] \simeq [V'_{Ag}])$ as $[e']$ does, while $[Ag_i^{\cdot}](\rightarrow K_F/[V'_{Ag}])$ and $[h^{\cdot}]$ decrease (see centre of Fig. 1 and curve 2 in the bottom picture). At lower temperatures short range interactions become important. This short range interaction can, to a good extent, be taken into account by an association reaction (see curve 3 in the bottom picture, low T) [17,18].

$$Cd_{Ag}^{\cdot} + V'_{Ag} \rightleftharpoons (Cd_{Ag}V_{Ag})^{\times}. \quad (8)$$

We now have three ionic species (free Cd^{2+}, free Ag^+-vacancy and associate) for which again, Boltzmann statistics can be applied with reasonable approximation.

Such a procedure does not work at high temperatures (usually below the melting point) at which so many native defects have been generated that (i) the restricted number of sites and (ii) the long-range interactions must be taken account of. The former can be done by using Fermi–Dirac type of statistics:

$$\mu = \mu^{\circ} + RT \ln \frac{c}{c_{max} - c} \quad (9)$$

the latter leads to the introduction of interaction coefficients (μ^{ex}) due to Coulomb interaction. These long-range Coulomb interactions lower the effective defect formation energy such that defect formation becomes successively more favourable leading to an over-Arrhenius increase of the ionic conductivity and eventually even to a phase transition (see curve 4 in the bottom picture, high T). The classical approach to describe long-range interactions is the Debye–Hückel theory [19] which fails at significantly high concentrations (>0.1%). In Ref. [20] it was shown that, in such cases, a quasi-Madelung approach ($\mu^{ex} \propto c^{1/3}$) can yield a reasonable explanation of both the conductivity anomaly as well as the phase transition temperatures. The proportionality factor between the excess chemical potential and the cube root of the concentration is in line with a simple Madelung estimate as well as with recent MD-simulations [21].

3. Equilibrium point-defect distribution at interfaces

Now we investigate the modifications due to approaching interfaces. First of all we adopt a simplified picture which assumes (ground) structural invariance up to the core of the interfaces which itself is thought to be of a different but invariant (ground) structure. In other words we assume the chemical ground structure to behave as an ideal step function and allow only the point-defect concentration to vary and to contribute to the adjustment of the electrochemical potentials.

Real structure = Perfect bulk structure
+ perfect core structure
+ inhomogeneous defect structure (10)

In particular, carrier mobilities and standard chemical potentials (and thus mass action constants) behave in a step-function way. In contrast to the perfect structure, the defect structure — and thus the carrier concentrations — does not vary in a step-function way but is smeared out around the interface.

We follow the core-space-charge model described in more detail in Ref. [22]. As a consequence of the abrupt change of structure and standard chemical potentials and as a consequence of the requirement

that the electrochemical potentials of all mobile species have to be homogeneous, changes of the chemical potentials occur at the expense of electrical potential changes, in other words, space charge regions with modified defect concentrations come into play. The complete treatment demands knowledge of defect chemistry of both bulk and core, to establish for each carrier j the relationship:

$$c_j = f_j(x; P, T, C; \mathbf{B}) \tag{11}$$

B denotes the parameter set additionally necessary to define the interface. Already in the case of an ideal grain boundary, **B** is at least a five-fold manifold[1] [24]. Owing to the kinetic constraints and the complexity of interfacial structure and composition, the core ground structure and composition (**B**) is more pragmatically handled as a irreversibly introduced boundary condition and thus as a further controlling parameter similar to C in Eq. (2).

If two majority defects 1, 2 of equal absolute charge follow the space charge field we can write

$$c_j/c_\infty = \left(\frac{1 + \vartheta_j \exp - x/\lambda}{1 - \vartheta_j \exp - x/\lambda}\right)^2. \tag{12}$$

ϑ, the degree of influence contains the boundary core chemistry, while c_∞ and $\lambda(c_\infty)$ contain the bulk chemistry. The conductance enhancement parallel to the interface follows as

$$\Delta Y^{\parallel} = \sum_{j=1,2} (2\lambda) F u_j \left(2c_\infty \frac{\vartheta_j}{1 - \vartheta_j}\right) \tag{13}$$

(u: mobility, $\vartheta_1 = -\vartheta_2$). For details see Ref. [25]. Besides grain boundaries, phase boundaries are of importance such as interfaces of a mixed conductor with an inert solid material, with a second mixed conductor (which includes grain boundaries) or with a gas phase. In Ref. [26] an extensive discussion of related conductivity effects is given. To mention a few examples, grain boundaries may exhibit conductive pathways along the enhancement layer while they may simultaneously block the transport by a resistive core; surface active insulators can adsorb mobile ions and lead to enhanced vacancy conduction; in the miscibility gap of two conductors, conductivity anomalies can occur through a carrier redistribution, and at surfaces adsorbed gas molecules may lead to ionic space charge effects (see Fig. 2: CaF_2/BF_3). Analogous effects are known for electronic conductors. In mixed conductors usually the interaction of the majority carriers (e.g. ions) defines the space charge potential which is then perceived by the minority species (e.g. electrons [26]). Beyond that, the ratio of ionic and electronic conductivity may be varied [28–30]. In some cases, surface-interaction free energies may well be enough to lead to interfacial phase transitions [31,32]. They can, e.g. be thought to be formed via charge carrier interaction as discussed which can be different in the boundary regions, e.g. due to modified carrier concentration [26].

Fig. 3 shows the conductivity enhancement of heterogeneously doped AgCl. The effects can be quantitatively described by an ideal space charge model [26].

The conductivity enhancement in heterogeneously doped β-AgI [33] is qualitatively in agreement with the simple space charge theory (tendencies, slopes etc.) but the absolute values are too high by orders of magnitude to account for the effect quantitatively. It has been shown [34–36] that interfacial phase transitions occur which are not unexpected in view of the polymorphism of the AgI-structures and the statements given in the previous section. A more detailed explanation of the anomaly is given in Section 4.

In addition to the excess charge, pure core disorder may also be important in view of lowered defect formation energies and varied mobilities for core defects. For more details on this see Ref. [37]. Recent computer simulations [38,39] show that in CeO_2 oxygen vacancies and excess electrons are more stable at the surface than in the bulk.

The step-function behaviour of the structure, i.e. of μ°, is of course an assumption. Structural models show that bond distances may vary over a certain range at boundaries in a more or less smooth way. From structure investigations it is known that the H_2O-structure of ice becomes water-like in the vicinity of surfaces [40], while the first layers of liquid water in contact with certain electrodes are

[1] Five is the number of macroscopic degrees of freedom determining the configuration of grain boundaries obtained by bringing together two single crystalline pieces. The additional microscopic degrees of freedom can usually not be controlled independently [23].

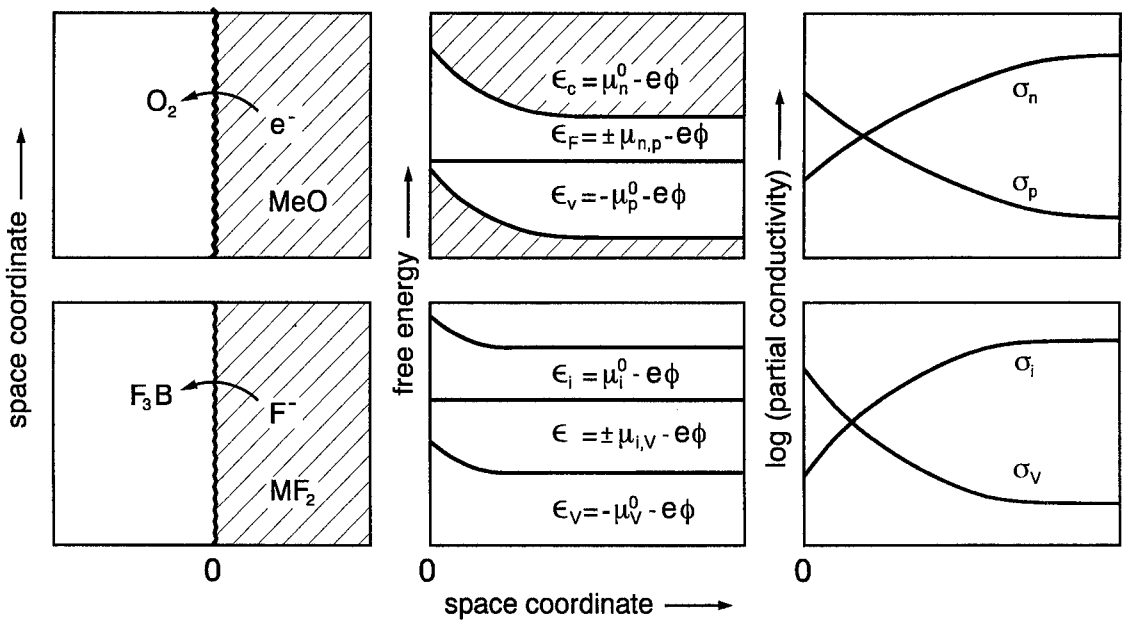

Fig. 2. The exposure of CaF_2 to the Lewis-acid BF_3 leads to an increase of the fluoride vacancy concentration (conductivity). The effect is analogous to the exposure of semiconducting oxides to O_2. This is shown by the potential diagrams in the central column (cf. Refs. [26,27]).

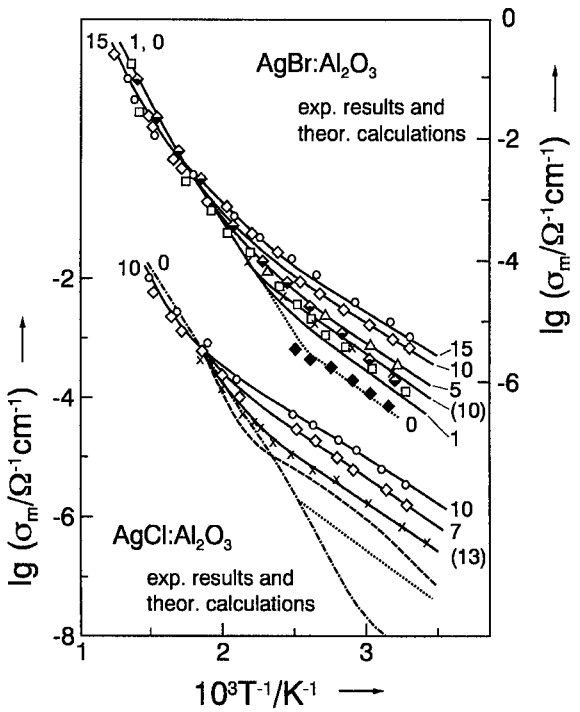

Fig. 3. The effect of 'heterogeneous doping' of AgCl and AgBr can be quantitatively interpreted by space charge effects [25].

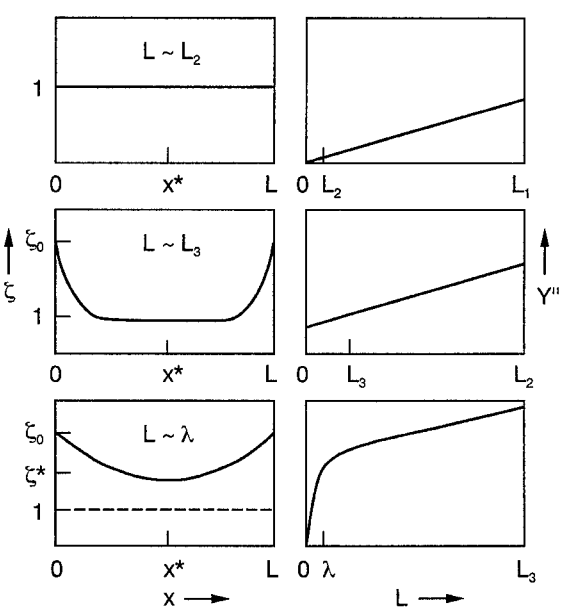

Fig. 4. The development of the mesoscopic space charge effect. L.h.s.: concentration profiles ($\zeta \equiv c/c_\infty$). R.h.s.: thickness dependence of the parallel excess conductance.

ice-like [41]. This point will be taken up again in Section 4.3. (Fig. 4).

4. Size effects on point-defect thermodynamics

4.1. 'Trivial' size effects

If the size of the crystal is reduced so is the distance between neighbouring interfaces, overall properties, e.g. the overall transport properties can significantly change just due to the increased interface to volume ratio, i.e. the local properties being invariant. Thus transport along the core regions may dominate in nanocrystalline samples although it may be completely insignificant in microcrystalline samples. The same is true for space charge transport. Nonetheless these 'trivial' effects can be striking [37]. One example is the depression of the melting point of nanosized crystals. This example is taken up again in Section 4.2. But let us now consider the situation that also the local properties are size-dependent.

4.2. Mesoscopic space charge effect

Again, we first adopt the abrupt structural model. Fig. 5 highlights the occurrence of a mesoscopic

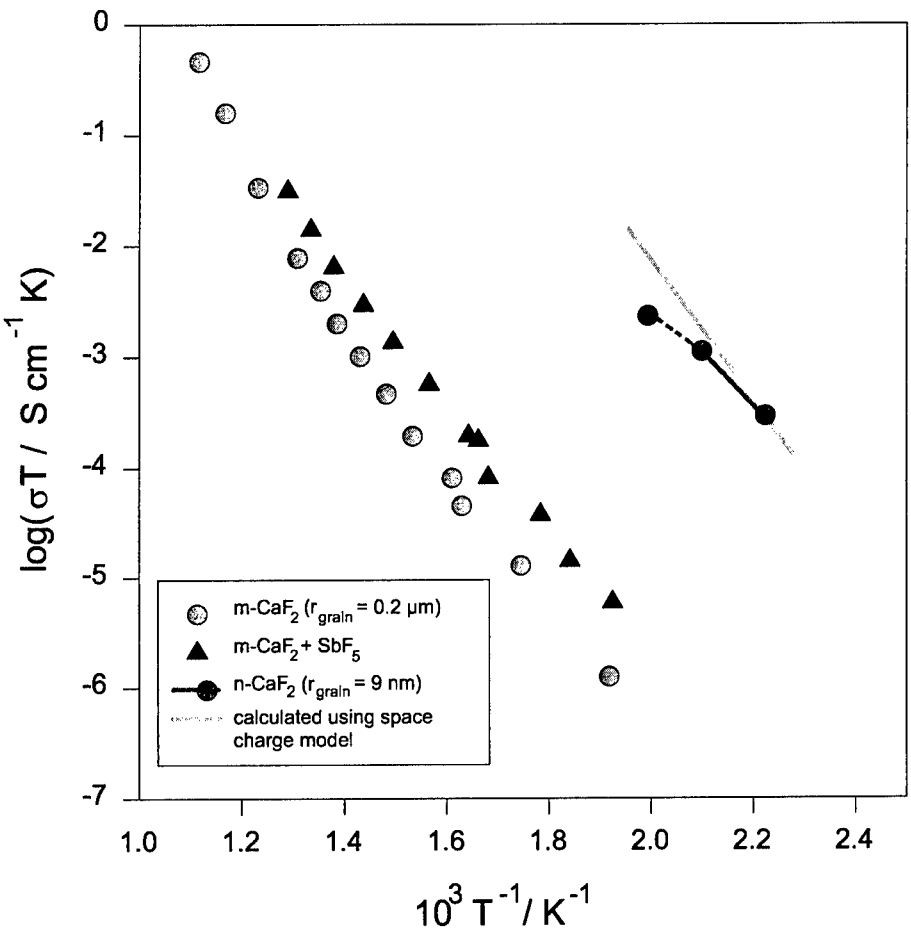

Fig. 5. Conductivity (without blocking grain-to-grain contacts) for nanocrystalline (n-) CaF_2 compared to coarse-grained (m-) CaF_2. The deflection of the data points at high T (n-CaF_2) indicates grain coarsening. Also shown are the conductivity data obtained by exposure of m-CaF_2 to the Lewis-acid SbF_5 (cf. also Fig. 2) [45,46].

effect if the sample thickness is no longer large compared with the Debye-length [42]. Then the space charge regions interfere, the sample is charged throughout, and in terms of conductivity an additional enhancement may occur for enrichment layers expressed by the nanosize factor (ns.f.) [43,44] [$c_0 \equiv c(x=0)$] (derived for a film!)

$$\text{n.s.f.} = \frac{4\lambda}{L}\left(\frac{c_0 - c^*}{c_0}\right)^{\frac{1}{2}} \tag{14}$$

where c^* is the concentration in the center of the symmetrical film and related to L and c_0 via:

$$\frac{L}{2\lambda} = 2\sqrt{c_\infty/c^*}\left[\mathscr{E}\left(\frac{c_\infty}{c^*}, \frac{\pi}{2}\right) - \mathscr{E}\left(\frac{c_\infty}{c^*}, \arcsin\sqrt{\frac{c^*}{c_0}}\right)\right] \tag{15}$$

$\mathscr{E}$ denoting elliptical integrals of the first kind, c_∞ being the bulk value. Even though predicted quantitatively more than a decade ago [43,44] clear experimental evidence for this is still lacking. The thickness-dependent conductance of thin LiI-films on sapphire could be nicely fitted by Eq. (14) [43,44], however it is probable that lateral inhomogeneities (island formation) obscure the picture. This is supported by a large apparent Debye-length obtained when a homogeneous situation is assumed [42,26].

Fig. 5 shows the high conductivity of nanocrystalline CaF_2 [45,46]. The conductivity can be explained by semi-infinite space charges. Owing to the high impurity content, the Debye-length can be assessed to be lower than the grain size of ~10 nm. In Ref. [47] the changed defect chemistry of nanocrystalline CeO_2 was explained by core effects. Also in this case, the sample thickness was still large compared to the Debye-length. Yet, a mesoscopic situation is certainly met in swollen Nafion or PEEK ion exchange membranes Fig. 6. There an organic backbone [per-fluorinated branched hydrocarbon network (Nafion)] or bundles of aromatic polyether ketones (PEEK) are separated by tiny water channels [48]. These organic backbones bear sulfonic acid groups. While the proton can be dissociated away, the anion is strongly bonded to the polymer. Since the thickness of the water channels is of the order of 1 nm and much lower than the Debye-length of water, these channels form mesoscopic space charge layers in which only very small gradients of the proton concentration exist. A systematic examination of the proton conductivity as the function of the separation thickness is necessary [49].

A further example is the already discussed conductivity enhancement in $AgI:Al_2O_3$ nanocomposites. As already outlined, the conductivities point towards space charge effects. However, a semi-infinite space charge model predicts too low an effect. Finite (mesoscopic) effects would require a lower grain size than estimated from the geometrical parameters. However, a recent structural analysis

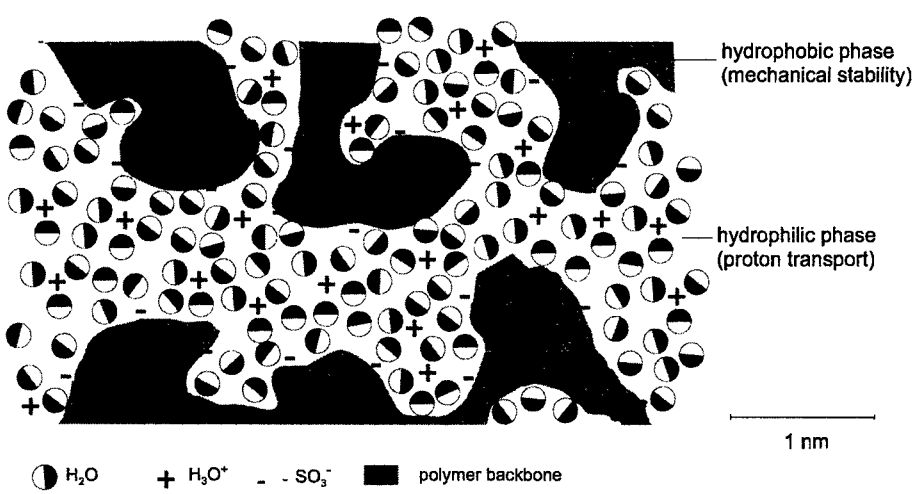

Fig. 6. Mesoscopic arrangement of acidified water channels in the PEEK polymers [48].

indicates the formation of a stacking fault structure formed at the interfaces (Fig. 7) [34]. This stacking fault sequence can also be conceived as a heterostructure in which β- and γ-layers alternate, the layer distance being of atomistic dimensions. If we can suppose an interfacial effect at the β/γ-boundary for which we have indications, a far-reaching ionic disorder is to be expected and the observed conductivity behaviour can be at least half-quantitatively explained. In this respect, more detailed investigations on such super-lattices are required as is the case in quantum well research.

Beyond electrical properties, such questions are important for stability considerations, as well as for kinetic (and in particular catalytic) properties. We

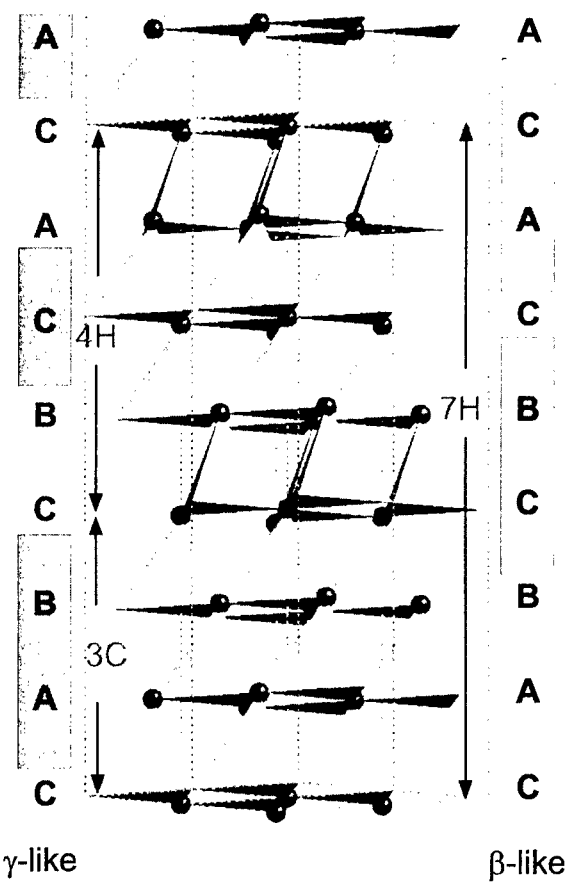

Fig. 7. Stacking fault (7H phase) forming at the Al_2O_3/AgI boundary, can be conceived as a β/γ/β/γ... sequence of (sub-) nanometre size leading to a pronounced disorder in the cation sublattice.

may mention (i) the fact, important for Li-batteries, that Li insertion into nanocrystalline hosts may not necessarily imply a homogeneous distribution of Li^+ and e^-, and (ii) the fact that drift effects in Taguchi gas sensors should be minimal, if $L \sim \lambda$, as the separation of the bulk and surface conductivity effects become almost irrelevant, and finally (iii) that pronounced size effects are expected for extent [47] and rate [50] of stoichiometric changes.

4.3. Mesoscopic structural effects

Now we are interested in potential size-dependencies of μ°, i.e. bending of (free) energy levels (apart from electrical field effects). For electronic levels, this can occur without structural effects just due to the extension of the electron's wave-function. The simple electron-in-the-box model indicates that the energy levels and hence also the energy differences depend on L and thus approximately

$$\Delta\mu^\circ \propto L^{-2}. \tag{16}$$

A clear example is illustrated by the colour changes exhibited by colloids as a function of size [51]. This dependence predicts a steep decay of this kind of level bending. Nano-electronics being concerned with nanoheterostructures, quantum wells, wires and dots relies on such confinement phenomena [4]. Similarly we expect confinement effects for protons but only under conditions where tunnelling is of relevance. In usual cases and in particular for larger ions, this is not the case. An extremely interesting topic is the exploration of nanosize effects in mixed conductors. In the case of typical ion conductors, a L-dependence of μ° implies structural changes. Then we must face the more complicated situation characterised by

$$\text{Real structure} = \text{Inhomogeneous perfect structure} + \text{(inhomogeneous) defect structure} \tag{17}$$

Experiments with NaCl clusters (Fig. 8) [6,7] show that the rock-salt structure is obtained already for small cluster sizes (> 10 molecular units). Minor variations in the bond lengths are then obviously not leading to a significant energetic effect: If we consider the energy and decompose the small crys-

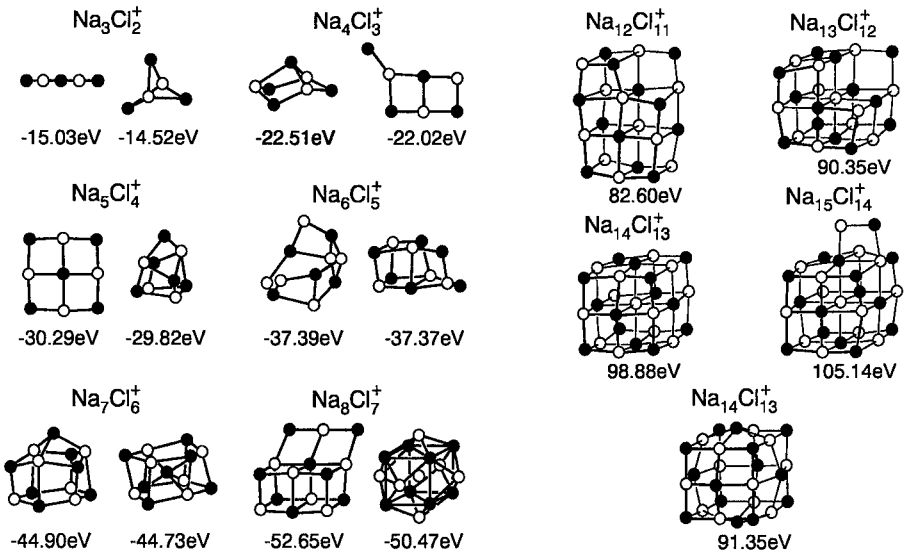

Fig. 8. Stable $(NaCl)_{n-1}$ Na^+-cluster according to Martin [6,7].

tals into 'bulk' and an outer shell of surface particles ('core') it turns out that the energies of the so-decomposed ground structures are quite invariant. More precisely, if surface and bulk energies are superimposed as $\alpha(L)N^{2/3} + \beta(L)N$, α and β are quite insensitive with thickness as the plot of $E/N^{2/3}$ vs. $N^{1/3}$ shows [52]. The situation seems to be similar in noble metals: The melting temperature changes of nanocrystalline Au particles are quite dramatic [53]. If the size of Au crystals is reduced to 20 Å, the melting point drops by 600 K. Nevertheless the effect can be understood by using only physical constants of massive gold [53], i.e. by trivial effects as denoted in Section 4.1. Note that for cubic clusters of 1000 atoms only half of the atoms are not sitting in surfaces. At smaller clusters also edge effects and corner effects become important. For a Wulff-crystal, the chemical potential correction ($\Delta\mu_{MX}$) compared to very large crystals is determined by $W \cdot V_m$, V_m being the molar volume and W the ratio of surface tension and distance between surface and centre which is the same for each plane. According to e.m.f. measurements [54], nanocrystalline copper shows an increase in the chemical potential which can be understood in this way.

Even though these findings cannot be generalised, it certainly will be, in many cases, a good approximation to state that such structural L-dependencies in μ° are restricted to extremely small sizes ℓ. Generally speaking, we expect a mesoscopic effect in the carrier concentration (i.e. in the mass action constants K) and in the conductivities (i.e. in both K and u) if $L \lesssim \ell$.

In cases in which the Debye-length is significant, we will then have to face two mesoscopic regimes as indicated in Fig. 9: an electrical one for $\lambda \gtrsim L \gg \ell$ and a structural one for $\ell \gtrsim L$. If ℓ is not small compared to λ, a complicated mixed behaviour occurs.

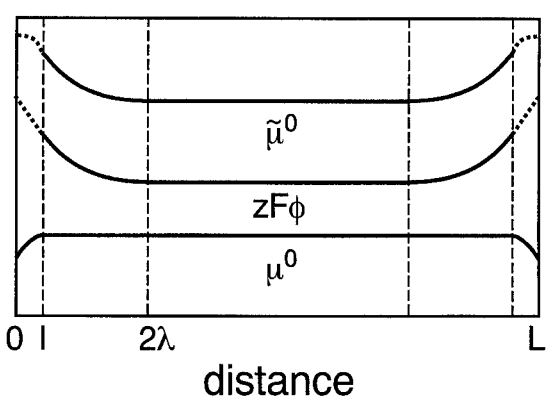

Fig. 9. If, at thicknesses smaller than ℓ, the structure changes, there is — in addition to space charge effects characterised by λ — a second size effect to be expected.

As outlined above, even with respect to the pure electrical effect not very much reliable data has been gathered. For the investigation of structural phenomena, this is even more true. Beyond that, conceptional problems still have to be solved as the question of the tensor character of the chemical potential if L becomes small. In addition, effects such as line and edge tension or triple junction properties may become highly relevant in nanosized samples. It is also worth mentioning that under those conditions the equilibrium crystal structure deviates from the Wulff-plot as it is also manifested in the individual equilibrium structure of small clusters. In short: even though a few conceptual points can be stated, the field of nano-ionics is largely terra incognita.

Acknowledgements

The author is indebted to H.L. Tuller for discussions and critical reading of the manuscript.

References

[1] B. Sakmann, E. Neher (Eds.), Single-channel Recording, Plenum Press, New York, 1995.
[2] R.J. Haug, K. von Klitzing, FED J. 6 (Suppl. 12) (1995) 4.
[3] K. von Klitzing, FED J. 4 (Suppl. 2) (1994) 2.
[4] K. von Klitzing, in: Max-Planck-Jahrbuch 1996, Verlag Vandenhoeck and Ruprecht, Göttingen, 1996, p. 111.
[5] A. Simon, Structure and Bonding 36 (1979) 81.
[6] T.P. Martin, Festkörperprobleme (Advances in Solid State Physics), Vieweg, Braunschweig XXIV (1984) 1.
[7] T.P. Martin, Phys. Reps. 95 (1983) 167.
[8] Nanostructured materials for energy applications, Y.-M. Chiang (Ed.), J. Electroceram. 1 (3) (1997).
[9] H.L. Tuller, Loc. Cit. (5) 211.
[10] J. Schoonman, Proceedings of the SSI-12-Conference, Thessaloniki, 1999, Solid State Ionics (2000) in press.
[11] C. Wagner, W. Schottky, Z. Physik. Chemie B11 (1930) 163.
[12] C. Wagner, Z. Physik. Chemie B32 (1936) 447.
[13] F.A. Kröger, Chemistry of Imperfect Crystals, North Holland, Amsterdam, 1964.
[14] G. Brouwer, Philips Res. Rep. 9 (1954) 366.
[15] J. Maier, Angew. Chem. Int. Ed. Engl. 32 (1993) 313.
[16] J. Maier, Angew. Chem. Int. Ed. Engl. 32 (1993) 528.
[17] N. Bjerrum, Kgl. Danske Videnskab. Selskab. Mat. Fys. Medd. 7 (1926) 3.
[18] A.B. Lidiard, in: S. Flügge (Ed.), Handbuch der Physik, Vol. 20, Springer, Berlin, 1957, p. 246.
[19] P. Debye, E. Hückel, Physik. Z. 24 (1923) 185.
[20] N. Hainovsky, J. Maier, Phys. Rev. B 51 (1995) 15789.
[21] F. Zimmer, P. Ballone, J. Maier, M. Parrinello, Ber. Bunsenges. Phys. Chem. 101 (1997) 1333.
[22] J. Jamnik, J. Maier, S. Pejovnik, Solid State Ionics 75 (1995) 51.
[23] A.P. Sutton, R.W. Balluffi, Interfaces in Crystalline Materials, Clarendon Press, Oxford, 1995.
[24] D. Wolf, in: D. Wolf, S. Yip (Eds.), Materials Interfaces. Atomistic-level Structure and Properties, Chapman and Hall, London, 1992, p. 1.
[25] J. Maier, J. Electrochem. Soc. 134 (1987) 1524.
[26] J. Maier, Prog. Solid State Chem. 23 (1995) 171.
[27] Y. Saito, J. Maier, J. Electrochem. Soc. 142 (1995) 3078.
[28] J. Maier, in: F.W. Poulsen, N. Bonanos, S. Linderoth, M. Mogensen, B. Zachau-Christiansen (Eds.), High Temperature Electrochemistry: Ceramics and Metals, Riso National Laboratory, Roskilde, Denmark, 1996, p. 67.
[29] J. Maier, Ber. Bunsenges. Phys. Chem. 93 (1989) 1468.
[30] J. Maier, Ber. Bunsenges. Phys. Chem. 93 (1989) 1474.
[31] R. Lipowsky, in: Phasenübergänge an Oberflächen (IFF Ferienkurs), FZ Jülich GmbH, Germany, 1993, p. 9.1.
[32] R. Lipowsky, Springer Tracts Mod. Phys. Vol. 127, in preparation.
[33] K. Shahi, J.B. Wagner, Appl. Phys. Lett. 37 (1980) 757.
[34] J.-S. Lee, St. Adams, J. Maier, Solid State Ionics, in press.
[35] N.F. Uvarov, E.F. Hairetdinov, A.I. Rykov, Yu.T. Pavlyukhin, Solid State Ionics 96 (1997) 233.
[36] J. Maier, J. Eur. Ceram. Soc. (2000) in press.
[37] J. Maier, Electrochem. (2000) in press.
[38] C.R.A. Catlow, R. James, W.C. Mackrodt, R.F. Stewart, Phys. Rev. B 25 (1982) 1006.
[39] C.R.A. Catlow, W.C. Mackrodt (Eds.), Computer Simulation of Solids, Lecture Notes in Physics, Vol. 166, Springer, Berlin, 1982.
[40] M. Elbaum, S.G. Lipson, J.G. Dash, J. Crystal Growth 129 (1993) 491.
[41] M. Vossen, F. Forstmann, A. Krämer, Solid State Ionics 94 (1997) 1.
[42] J. Maier, Solid State Ionics 23 (1987) 59.
[43] J. Maier, Solid State Ionics 23 (1987) 59.
[44] J. Maier, S. Prill, B. Reichert, Solid State Ionics 28–30 (1988) 1465.
[45] W. Puin, P. Heitjans, W. Dickenscheid, H. Gleiter, Defects in Insulating Materials, in: O. Kanert, J.-M. Spaeth (Eds.), World Scientific, Singapore, 1993, p. 137.
[46] W. Puin, S. Rodewald, R. Ramlau, P. Heitjans, J. Maier, Solid State Ionics 131 (2000) 159–164.
[47] Y.-M. Chiang, E.B. Lavik, I. Kosacki, H.L. Tuller, J.Y. Ying, J. Electroceram. 1 (1997) 7.
[48] K.D. Kreuer, in: B.V.R. Chowdari, K. Lal, S.A. Agnihotry, N. Khare, S.S. Sekhon, P.C. Srivastava, S. Chandra (Eds.), Solid State Ionics: Science and Technology, World Scientific Publishing Co, Singapore, 1998, p. 263.
[49] M. Ise, PhD Thesis, University of Stuttgart, 2000.
[50] J. Jamnik, J. Maier, J. Electrochem. Soc. 145 (1998) 1762.
[51] A. Henglein, Ber. Bunsenges. Phys. Chem. 101 (1997) 1562.
[52] H.G. Fritsche, Phys. Stat. Sol. (b) 154 (1989) 603.
[53] Ph. Buffat, J.-P. Borel, Phys. Rev. A 13 (1976) 2287.
[54] Ch.P. Gräf, U. Heim, G. Schwitzgebel, Solid State Ionics 131 (2000) 165–174.